Title	Multiple frequency band and high isolation mobile device antennas using a capacitive slot
Author(s)	ROWELL, CR; Lam, EYM
Citation	IEEE Transactions on Antennas and Propagation, 2012, v. 60 n. 8, p. 3576-3582
Issued Date	2012
URL	http://hdl.handle.net/10722/185907
Rights	IEEE Transactions on Antennas and Propagation. Copyright © IEEE

Multiple Frequency Band and High Isolation Mobile Device Antennas Using a Capacitive Slot

Corbett Rowell, *Member, IEEE*, and Edmund Y. Lam, *Senior Member, IEEE*

***Abstract*—The performance characteristics of the capacitive slot, or a slot placed between the feed and ground connections, in a planar inverted-F antenna (PIFA) are comprehensively analyzed. The PIFA capacitive slot behavior is measured inside a two antenna system within a mobile phone where the first antenna is a multiple band PIFA and the second antenna is a higher frequency band PIFA directly overlapping with the first antenna higher frequency band. The dual band PIFA in this paper is designed to be resonant in the quad-band GSM + $3G/4G$, and the second PIFA is resonant in the 3G/4G frequency bands. The capacitive slot has three types of behaviors: affect the matching of existing frequency resonances, induce another frequency resonance, and improve the isolation between the two antennas. Together with optimal antenna ground and feed placement, the capacitive slot can act as a notched bandstop filter to decrease the S_{21} mutual coupling between the two antennas by over 20 dB and decrease the envelope correlation by almost one order of magnitude.**

***Index Terms*—Antenna efficiency, antenna theory, bandstop filters, inverted-F antennas, isolation technology, microstrip antennas, mobile antennas, multiple input multiple output (MIMO) systems, mutual coupling, scattering parameters.**

I. Introduction

MULTIPLE frequency band operation and isolation between small antennas are two critical factors in many practical applications, especially mobile phones and MIMO (multiple input multiple output) terminal devices, affecting the coupling, the S-parameters, the radiation efficiency, and the channel capacity. Mobile phones are integrating more standards into the device, such as GSM, 3G, 4G, Wifi, Bluetooth, digital TV, etc., with a design requirement of a small device form-factor. This requires antennas with not only multiple frequency bands, but good antenna isolation to reduce the signal coupling, increase channel capacity, and increase the overall performance of the device. MIMO systems have attracted significant commercial interest due to the potential of achieving significant increases in wireless channel capacity and are currently being implemented as part of the 4G standards (Long Term Evolution-LTE) [1].

It is difficult to achieve good isolation in a design requiring closely-packed antennas. For PIFA antennas, several papers have stated that it requires inter-antenna spacing of at least half a wavelength in order to achieve greater than 20 dB isolation [2]–[4]. Over the past decade, researchers have devised a variety of techniques for increasing the isolation to over for 2–3 closely packed (separation $<\lambda/8$) small antennas that operate at a single frequency band using PCB and antenna modifications.

PCB modifications include mushroom-like electronic bandgap (EBG) structures [5] and defected ground-plane structures (DGS) [6], [7] to suppress the surface wave between the two antennas, thus reducing the mutual coupling. The EBG structures require a large surface area beneath the antenna and the DGS structures modify the PCB by cutting slots into the PCB. Both techniques create difficulties for RF circuits to feed the antenna and for other device modules to use the PCB area beneath and adjacent to the antennas. Antenna modifications are mostly parasitic based with the creation of a parasitic strip that is either directly connected to the antennas via a neutralization line [8] or capacitively coupled to the antennas [9]. The neutralization line can be applied to either two single band antennas at the same frequency or two single band antennas with a frequency overlap, such as one antenna for GSM1800 and the second antenna for 3G UMTS [10].

In addition to MIMO and diversity antenna systems where all the antennas operate on the same frequency bands with identical or symmetric antenna geometry, there is a growing need for antenna systems where one antenna has multiple frequency bands and the other antennas are single banded. One example is a GSM plus LTE antenna system where the GSM standard only requires a single antenna and the LTE standard requires 2 antennas for MIMO operation. In this case, the first antenna would be a GSM plus LTE antenna and the secondary antenna would be a dedicated LTE antenna.

This paper analyzes an antenna modification of a long slot between the ground and feed locations (labeled as a capacitive slot) in one of the antennas within a two antenna element system. Although the capacitive slot's matching and resonance properties at a single frequency band have been studied in [11], the isolation effect of the capacitive slot has not been fully analyzed. The antenna geometry discussed in [12] uses two slots to provide isolation and quad-band GSM frequency resonances, but the presentation did not perform a comprehensive analysis of the capacitive slot's matching, resonance, and isolation characteristics. It is further shown that the proper placement of the ground and the feed together with the slot create a bandstop filter, decreasing the mutual coupling in the bandstop frequency band significantly.

The antenna design and geometry is presented in Section II and the methodology used to analyze and measure the antenna

Manuscript received March 21, 2011; manuscript revised September 22, 2011; accepted April 02, 2012. Date of publication May 23, 2012; date of current version July 31, 2012.

C. Rowell is with the University of Hong Kong and Applied Science and Technology Research Institute (e-mail: corbett@astri.org).

E. Y. Lam is with the University of Hong Kong, Pokfulam, Hong Kong.

Color versions of one or more of the figures in this paper are available online at http://ieeexplore.ieee.org.

Digital Object Identifier 10.1109/TAP.2012.2201077

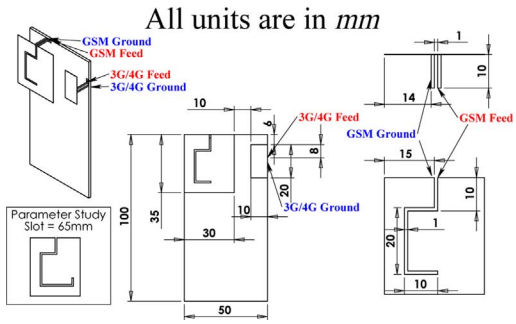

Fig. 1. Antenna and PCB geometry for the C-slot of length $l = 50$ mm in the dual-band PIFA where the feed and the ground connections are on opposite sides of the slot with width of 1 mm.

properties is discussed in Section III. The results of the antenna measurements are discussed in Section IV with a conclusion briefly summarizing the paper in Section V.

II. Antenna Design and Geometry

This paper analyzes a slot geometry where the slot is a C-shaped meandering slot (or C-slot) as shown in Fig. 1. Port 1 is a dual-band PIFA antenna of length 35 mm and width of 30 mm for the $0.8-1.0$ GHz and the $1.7-2.2$ GHz frequency bands (can also be considered a quad-band PIFA), and a second PIFA antenna for the 3G/4G frequency bands $(1.7-2.2\ \text{GHz})$. The dual-band PIFA in this paper has one slot resonance created by the slot (f_{slot}) and one PIFA resonance (f_{PIFA}) at [13]: $\lambda_{PIFA} = 4(L_{PIFA} + W_{PIFA} + H_{PIFA})$.

A slot is cut between the ground and feed connections of the dual-band PIFA antenna with a slot width of $w = 1$ mm. It is often labeled as a capacitive slot in literature [11] since it increases the shunt capacitance of the antenna. It will be shown in this paper that when the capacitive slot is lengthened, it changes both the capacitance and the inductance of the antenna, forming a bandstop filter and leading to an increase in isolation between the two antennas. The dual-band PIFA feed is placed to the right of the slot and is labeled RHF (right-hand feed) with the ground connection to the left of the slot and the left-hand feed (LHF) orientation places the feed on the left side of the slot with the ground connection to the right of the slot. The separation between the two antennas is $s = 10$ mm, or $\lambda/16$ at 1.9 GHz. The antenna height is set at $d = 10$ mm in order to decrease the effect of measurement tolerances in the higher field densities associated with lower heights. The base PCB size is set at a length of 100 mm and a width of 50 mm, similar to most mobile phones in the market.

For independent analysis of the capacitive slot, additional slots or parasitics are not used in this paper; though for quad-band and penta-band antenna systems, an inductive slot or parasitic element [14] would be helpful to create a wideband frequency resonance in the 2 GHz frequency band.

In the parameter study, the slot length is changed from $l_{slot} = 0$ mm to $l_{slot} = 65$ mm in 5 mm segments to illustrate the effect on the antenna matching, slot resonance, and isolation properties.

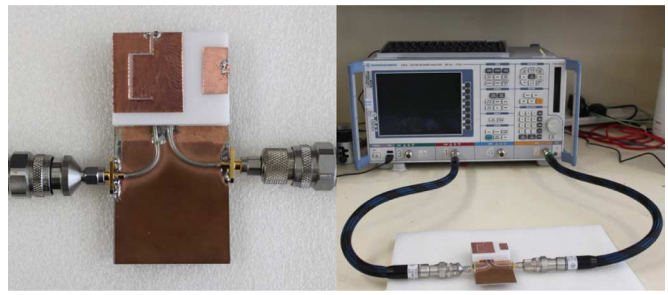

Fig. 2. Antenna and PCB prototype.

III. Measurements & Methodology

A. Measurements

Prototypes were constructed using FR4 PCB, copper tape, and a plastic ABS antenna carrier of dielectric constant $\epsilon_r = 3.0$ (Fig. 2). The S-parameters were measured after adjusting for the correct phase delay due to the measurement cables. The Z-parameters were directly calculated from the S-parameter measurements, assuming a characteristic cable impedance of $Z_0 = 50\ \Omega$. Both a Rohde & Schwarz ZVB network analyzer and an Agilent E5071C network analyzer were used for the S-parameter measurements.

For the passive antenna radiation efficiency measurements, the RF cable is routed through the PCB prototype and exits the PCB in an area that causes the least disturbance to the electromagnetic field distribution of the antenna (typically in the center of the PCB since the current distribution will often be high at both ends of the PCB). Port 2 is terminated by a 50 Ohm load when measuring Port 1 and visa versa for the Port 2 measurement. A Satimo Starlab system [15] was used to measure the total antenna radiation efficiency η and the 2-D antenna gain.

B. Circuit Model of the Capacitive Slot

A slot cut transversely into a microstrip line can be modeled as a series *RLC* circuit with the series inductance as the dominant effect [16]. The capacitive effects are considered negligible and the series inductance can be calculated as an empirical function dependent on the ratio of the characteristic impedance of the microstrip line and the slot impedance

$$L\left(\frac{\text{nH}}{\text{mm}}\right) = 2h\left(1 - \frac{Z_0\sqrt{\epsilon_e}}{Z_{slot}\sqrt{\epsilon_{slot}}}\right)^2 \tag{1}$$

where Z_0 is the characteristic impedance of a microstrip line of width W, Z_{slot} is the characteristic impedance of the microstrip line adjacent to the slot of width $(W - l_{slot})$, h is the height of the microstrip line, and ϵ_e is the effective dielectric constant for the microstrip line and ϵ_{slot} is the effective dielectric constant for the microstrip line adjacent to the slot

$$\epsilon_e = \frac{\epsilon_r + 1}{2} + \frac{\epsilon_r - 1}{2}\frac{1}{\sqrt{1 + \frac{12h}{W}}}. \tag{2}$$

The effect of the series inductance is similar to inductive loading properties of a slot cut into a PIFA where both the feed and ground connections are on the same side of the slot.

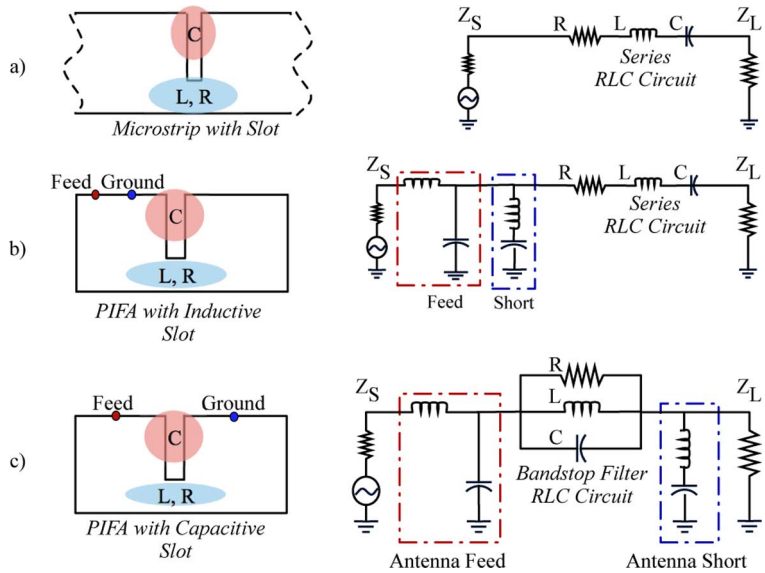

Fig. 3. Equivalent circuit for a microstrip line with a slot and a PIFA with slot. The physical representation of the slot shows the location of the capacitance and inductance/resistance that forms the *RLC* bandstop filter equivalent circuit. The capacitances in the feed and the ground are the fringing electrical fields from antenna edges.

When the slot is cut between the ground and the feed, the antenna isolation properties are similar to a bandstop filter, suggesting the equivalent circuit is not a series *RLC* circuit, but instead is a parallel *RLC* circuit (Fig. 3). The equivalent parallel inductance and capacitance can be calculated using (1), the resonant frequency of a parallel LC circuit $\omega_0^2 = 1/LC$, and low-pass filter series inductance to parallel inductance and parallel capacitance transformation [17]

$$L_p = \frac{\omega_c L_s Z_0 \Delta}{\omega_0} \tag{3}$$

$$C_p = \frac{1}{\omega_0^2 L_p} \tag{4}$$

where $\Delta = (\omega_2 - \omega_1)/\omega_0$, ω_c is the radian cutoff frequency for the low pass filter (assumed to be ω_1), $\omega_2 - \omega_1$ is the radian bandwidth (3 dB below peak resistance), and ω_0 is the resonance frequency (assumed to be the peak resistance for $|Z_{11}(\omega)|$).

C. Group Delay

The parallel *RLC* circuit forms a bandstop filter with a notch at the S_{21} antiresonance and is often characterized as having high group delay in that region. Group delay is normally used for filter design to characterize the distortion of a broadband signal inside the filter and is also an important parameter for the design of UWB and GPS antennas since some UWB/GPS systems are very sensitive to signal timing and phase distortions [18], [19].

The group delay is the negative derivative of the phase response as a function of frequency

$$S'_{21} = -\frac{\partial S_{21\angle}}{\partial f} \tag{5}$$

where $S_{21\angle}$ is the unwrapped phase response.

In addition to measuring the signal distortion, group delay can be used to characterize the S_{21}, or mutual coupling between antennas. Antenna structures with a very sharp S_{21} antiresonance at particular frequencies (i.e., $S_{21} < -30$ dB) [7], [9] all have a group delay at that frequency that is much greater than for the rest of the signal bandwidth, indicating that part of the antenna geometry acts as a bandstop filter.

IV. Results

A. No Slot & Capacitive Slot

The Port 1 dual-band PIFA without the slot is resonant at 0.95 GHz ($S_{11} = -25$ dB) and 3.37 GHz ($S_{11} = -4$ dB) with peak efficiencies of 82% and 43%, respectively. When a slot of length $l_{slot} = 50$ mm is placed between the feed and the ground connections of the Port 1 PIFA, the slot does not shift the first resonance at 0.95 GHz, but changes the matching at the lower frequency band, resulting in a worse $S_{11} = -9$ dB. The slot forms a third resonance at $f_{slot} = 1.86$ GHz ($S_{11} = -8$ dB). In addition, the slot forms a bandstop antiresonance at $f_{BSF} = 1.86$ GHz ($S_{21} = -40$ dB.) At a slot length of $l_{slot} = 50$ mm, the peak group delay is at 15 ns, compared to less than 2 ns for a slot length of 0 mm. The radiation patterns are relatively unchanged for the PIFA without the slot and PIFA with the slot. The slot effects on the Port 1 PIFA are illustrated in Figs. 4–6 and 11.

The frequency resonance and radiation properties of the 3G/4G single-band PIFA antenna at Port 2 are not affected by the change of the slot geometry with an average peak efficiency of 77% at 1.94 GHz ($S_{11} = -15$ dB) for all slot lengths and 2-D radiation patterns that are unchanged (Fig. 11).

This paper uses the S-parameters [20], to calculate ρ_{12}:

$$\rho_{12} = \frac{\left|S_{11}^* S_{12} + S_{21}^* S_{22}\right|^2}{\left(1 - |S_{11}|^2 - |S_{21}|^2\right)\left(1 - |S_{22}|^2 - |S_{12}|^2\right)} \tag{6}$$

where ρ_{12} is the envelope correlation between the antenna at Port 1 and the antenna at Port 2. The average envelope correlation ($\bar{\rho}_{12}$) between 1.8 – 2.0 GHz for a PIFA with a 50 mm slot was $\bar{\rho}_{12} = 0.02$. Although the PIFA without the slot did

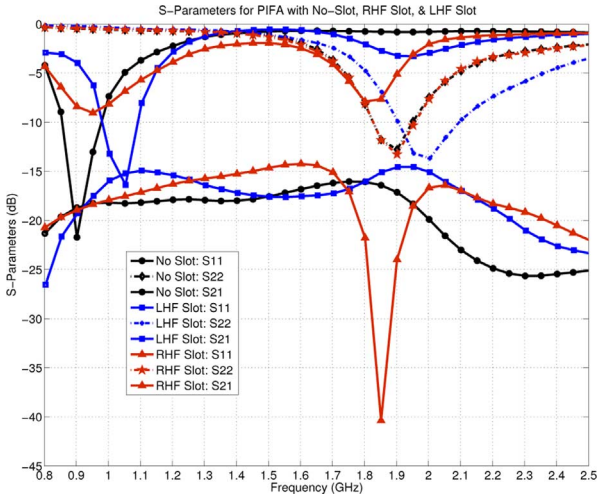

Fig. 4. S-Parameters comparison between PIFA without slot and PIFA with slot for both RHF and LHF geometries.

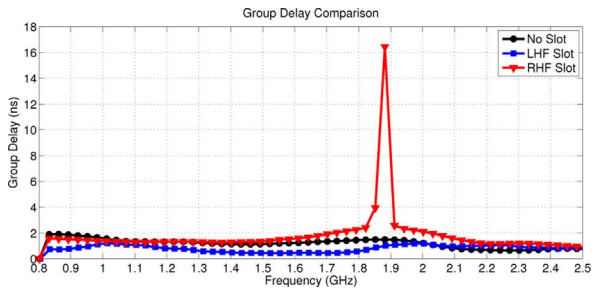

Fig. 5. Group delay comparison between PIFA without a slot and PIFA with slot for both RHF and LHF geometries: The RHF geometry has a group delay of 16.5 ns; whereas the no slot and LHF geometries have a group delay of less than 2 ns.

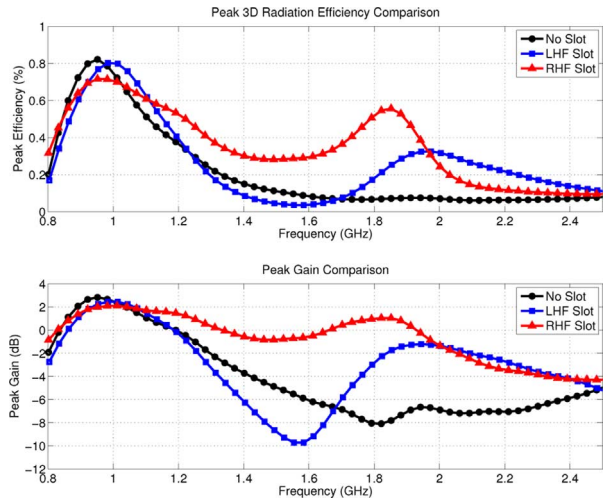

Fig. 6. Antenna 1 PIFA peak gain & efficiency comparison between no slot and slot length $= 50$ mm with LHF and RHF geometries.

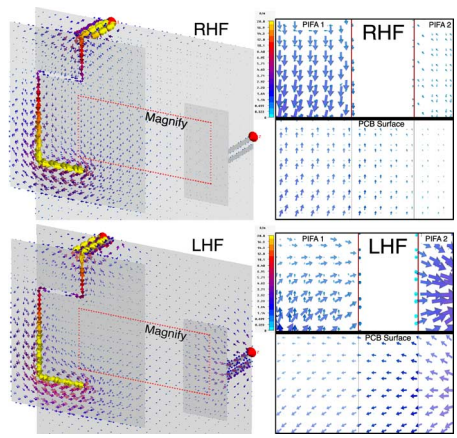

Fig. 7. Surface current distributions for RHF and LHF antenna geometries at $f = 1.86$ GHz and a phase of 0 degrees. The magnified surface current distribution is illustrated on the right for both the antenna and PCB surfaces. The current density is normalized to 20 A/m for comparison.

not have a second resonance in the higher frequency band, its average envelope correlation in the same frequency band was much higher at $\bar{\rho}_{12} = 0.15$.

1) Feed Placement: The slot matching properties and resonance exist for both feed and ground placements of right-hand feed (RHF) and left-hand feed (LHF). The bandstop antiresonance characteristic, however, is dependent on the placement of the feed and the ground. If the Port 2 antenna is located to the right of the Port 1 antenna, then a feed placed to the right of the slot with the ground to the left of the slot, labeled RHF, forces the Port 1 current to flow across the slot towards Port 2, creating the bandstop filter effect.

Fig. 4 compares the S-parameters with a slot length of 50 mm to show the difference between using the LHF and the RHF antenna geometries. The LHF geometry has no bandstop filter effect at 1.86 GHz where $S_{21} = -15$ dB and the capacitive slot with a RHF geometry has higher isolation properties with a bandstop antiresonance of $S_{21} = -42$ dB at 1.86 GHz. The effect of the feed and ground placement also manifests in the antenna efficiency and the 2-D radiation patterns as shown in Figs. 6 and 11. The RHF geometry increases the in-band radiation efficiency from 33% for the LHF geometry to 55% due primarily to the LHF S_{11} mis-match (the antenna isolation only has an effect on total efficiency when $S_{21} > -10$ dB with a 50% reduction in efficiency at $S_{21} = -5$ dB [12]). Despite the LHF S_{11} mis-match in the higher frequency band, its average envelop correlation between $1.8 - 2.0$ GHz was $\bar{\rho}_{12} = 0.06$, or three times higher than the average envelope correlation for the RHF.

The surface current distributions at $f = 1.86$ GHz (slot resonance and bandstop antiresonance) are illustrated in Fig. 7 using CST Microwave Studio where the PCB and antenna are modeled as perfect conductors. The LHF geometry has currents on the PCB and antenna surface flowing towards antenna 2 and consequently no bandstop antiresonance. The RHF geometry effectively re-phases the antenna and PCB surface current by 90 degrees in the magnified region and 180 degrees near the capacitive slot, resulting in a bandstop antiresonance.

The remainder of the paper examines the matching, resonance, and isolation properties of the RHF antenna geometry.

B. Parameter Study: Slot Length

As the slot length increases, $|Z_{11}(\omega)|$ in the lower band increases and both the slot resonance and the bandstop antiresonance decrease in the higher band. The equivalent parallel in-

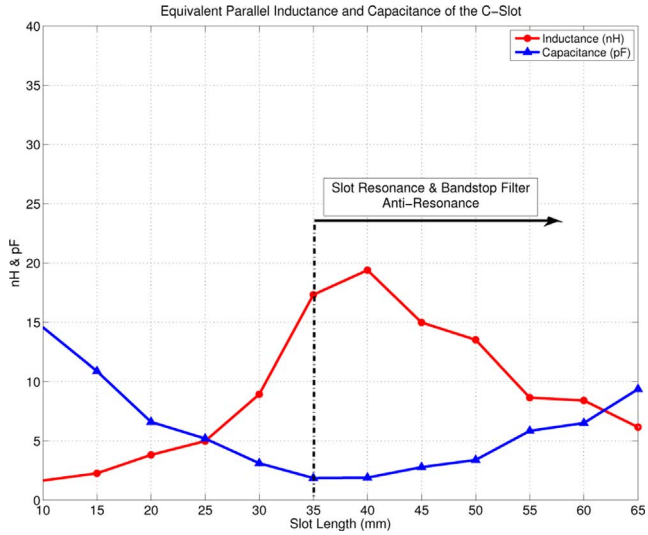

Fig. 8. Equivalent capacitance and inductance of the slot.

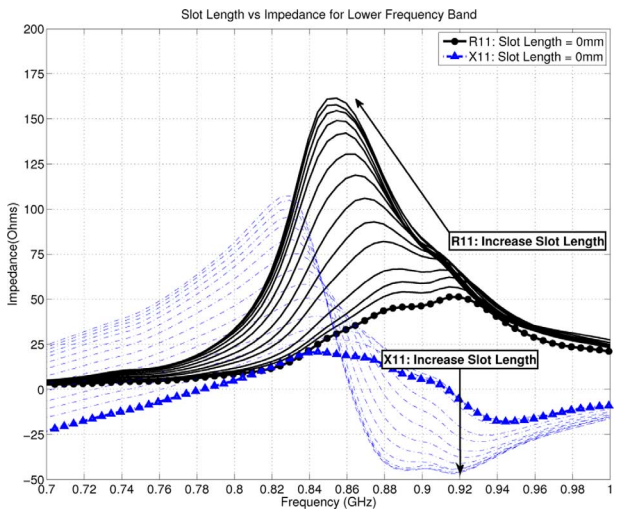

Fig. 9. Effect of slot length on antenna impedance: As slot length increases, R_{11} increases, and the Z_{11} resonance at $X_{11} = 0$ decreases by 54 MHz.

ductance and capacitance is calculated from (1)–(4) and presented in Fig. 8. For the C-slot, the parallel capacitance actually decreases until a critical slot length of $l_{slot} = 30$ mm, at which point the parallel capacitance starts to increase. This is consistent with the slot's physical behavior where the slot resonance and bandstop filter properties only appear after $l_{slot} = 30$ mm. In the higher frequency band, the slot has a separate resonance that becomes prominent after the slot length is increased over 30 mm. There is a separate bandstop resonance that also becomes more dominant for slot lengths over 30 mm with an increase in group delay from < 2 ns for $l_{slot} < 30$ mm to 7 ns at $l_{slot} = 30$ mm to 16.5 ns at $l_{slot} = 50$ mm.

1) Capacitive Slot Matching Properties: The capacitive slot changes the matching parameters of the PIFA frequency band of the dual band PIFA as discussed in [11]. Fig. 9 shows the effect of the slot length on the impedance where an increase in slot length decreases the impedance resonant frequency (defined where the reactance $X_{11} = 0$) by a small amount and increases the resistance R_{11}. The peak R_{11} at $X_{11} = 0$ increases

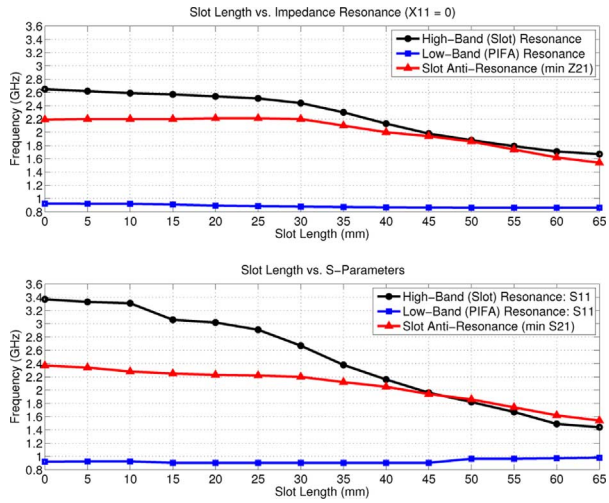

Fig. 10. Impedance resonance and S-Parameters (50 Ω) as functions of slot length.

at roughly 2 Ω/mm from 47 Ω at a slot length of 0 mm to 147 Ω at a slot length of 50 mm. At $l_{slot} = 50$ mm, the peak resistance only increases at 1 Ω/mm, suggesting an asymptotic limit.

The 50 Ω matched resonant frequency for the first antenna, f_{PIFA}, is 950 MHz, with a radiation efficiency between 70–80%, and the a VSWR<3.0 (50 Ω matching) bandwidth between 20–30%. At 920 MHz, the reactance decreases from -5.5 Ω at a slot length of 0 mm to -44 Ω at a slot length of 50 mm. A similar asymptotic effect appears at $l_{slot} = 50$ mm where the minimum reactance is constant at -46 Ω for slot lengths over 55 mm.

The radiation efficiency for the PIFA low-band resonance decreases from 82% ($l_{slot} = 0$ mm) to 70% ($l_{slot} = 50$ mm) at a rate of -2% per 10 mm slot length.

The capacitive slot does not affect the matching at the higher frequency band, but forms a new resonance, as discussed in the following section.

2) Capacitive Slot Resonance Properties: In addition to the PIFA resonance, the slot itself radiates (as illustrated in Fig. 7 with a strong surface current on the inside edges of the slot) and creates a second resonance in the higher frequency band. The low-band f_{PIFA} impedance resonance is relatively constant for different slot lengths with a decrease of 54 MHz from slot length of $l_{slot} = 0$ mm to $l_{slot} = 65$ mm, whereas the high-band f_{slot} resonance decreases by almost 1 GHz from slot length of $l_{slot} = 0$ mm to $l_{slot} = 65$ mm (Fig. 10).

The frequency resonance occurs after a slot length of 30 mm and has an electrical length between $\lambda/3 - \lambda/2$. The change in resonant length is due to the increased loading as the slot inductance increases with longer length with the slot resonance electrical length converging to $\lambda/3$. The radiation efficiency for the slot resonance is between 60–70% for 20 mm $< l_{slot} <$ 50 mm and 50–55% for $l_{slot} > 50$ mm.

3) Capacitive Slot Isolation Properties: When the slot length is longer than 30 mm, the slot forms a bandstop filter with an antiresonance determined by the capacitance and inductance of the slot, as illustrated in the equivalent circuit (Fig. 3). After

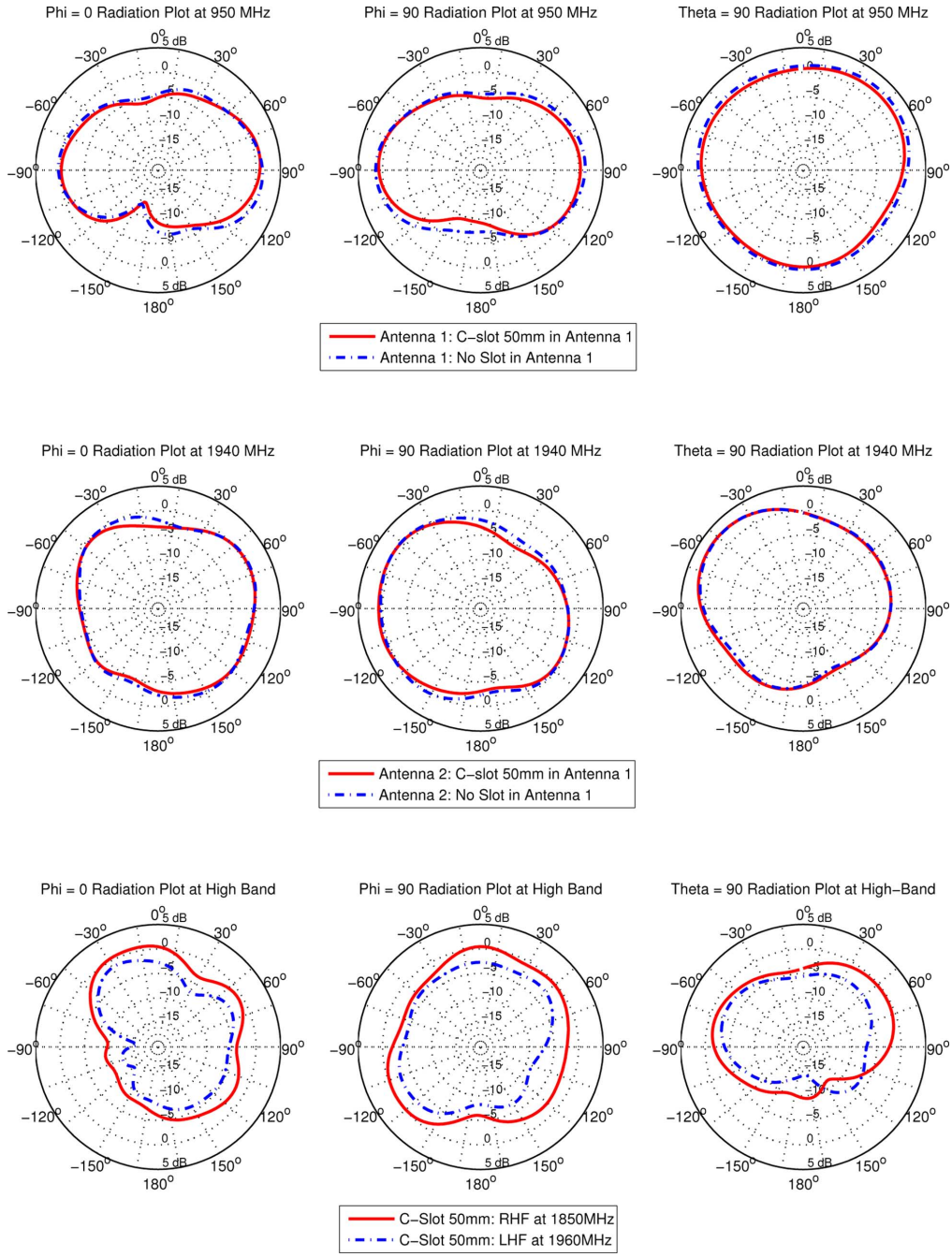

Fig. 11. Three cut antenna gain patterns: Slot vs No-Slot for port 1 antenna, slot vs No-Slot for port 2 antenna, and RHF vs LHF for port 1 antenna with a slot at respective frequency resonances.

30 mm of slot length, the S_{21} bandstop antiresonance (f_{BSF}) decreases at roughly 20 MHz per mm.

The bandstop antiresonance can be further fine-tuned by either placing additional ground connections (changing the antenna inductance) or by widening the slot (changing the antenna capacitance). After placing a second ground connection at the top left corner of the antenna, the slot the bandstop antiresonance increased by 16%. The antenna efficiency in the high-band (slot resonance) improved from 55% to 70% due to improved matching from the second ground connection. After widening the slot from 1 mm to 2 mm, the bandstop antiresonance increased by 2%.

V. Summary & Conclusions

In this paper, the resonance, matching, and isolation properties of the capacitive slot inside shorted microstrip antennas were analyzed. The slot creates an additional resonance within the PIFA and can be easily adjusted to the desired frequency. By placing the feed to the right of the slot and the ground on the opposite side, a bandstop filter is created, reducing the S_{21} inside the stop band by over 20 dB. By optimizing the slot parameters, diversity, MIMO, and combined GSM plus 3G/4G antennas can be constructed with very low coupling, low enve-

lope correlation, wide bandwidth, and high efficiency in limited space within mobile terminals.

REFERENCES

[1] *"Technical specification group radio access Network; user equipment (UE) radio transmission and reception (FDD/TDD),"* ver. (release 9), Third Generation Partnership Project (3GPP), TS 25.101/102/104/105 V9.5.0, 2010.

[2] H. Carrasco, H. D. Hristov, R. Feick, and D. Cofre, "Mutual coupling between planar inverted-F antennas," *Microw. Opt. Technol. Lett.*, vol. 42, no. 3, pp. 224–227, Aug. 2004.

[3] T. Taga and K. Tsunekawa, "Performance analysis of a built-in planar inverted F antenna for 800 MHz band portable radio units," *IEEE J. Sel. Areas Commun.*, vol. SAC-5, pp. 921–929, Jun. 1987.

[4] K. Tsunekawa and K. Kagoshima, "Analysis of a correlation coefficient of built-in diversity antennas for a portable telephone," in *Proc. AP-S. Merging Technologies for the 90's Dig.*, May 1990, vol. 1, pp. 543–546.

[5] F. Yang and Y. Rahmat-Samii, "Microstrip antennas integrated with electromagnetic bandgap (EBG) structures: A low mutual coupling design for array applications," *IEEE Trans. Antennas Propag.*, vol. 51, no. 10, pp. 2936–2946, Oct. 2003.

[6] D. Ahn, J.-S. Park, C.-S. Kim, J. Kim, Y. Qian, and T. Itoh, "A design of the low-pass filter using the novel microstrip defected ground structure," *IEEE Microw. Theory Tech.*, vol. 49, no. 1, pp. 86–93, Jan. 2001.

[7] C.-Y. Chiu, C.-H. Cheng, R. D. Murch, and C. R. Rowell, "Reduction of mutual coupling between closely-packed antenna elements," *IEEE Trans. Antennas Propag.*, vol. 55, no. 6, pp. 1732–1738, Jun. 2007.

[8] A. Diallo, C. Luxey, P. Le Thuc, R. Staraj, and G. Kossiavas, "Enhanced two-antenna structures for universal mobile telecommunications system diversity terminals," *Microw. Antennas Propag., IET*, vol. 2, no. 1, pp. 93–101, Feb. 2008.

[9] A. C. K. Mak, C. R. Rowell, and R. D. Murch, "Isolation enhancement between two closely packed antennas," *IEEE Trans. Antennas Propag*, vol. 56, no. 11, pp. 3411–3419, Nov. 2008.

[10] A. Diallo, C. Luxey, P. L. Thuc, R. Staraj, and G. Kossiavas, "Study and reduction of the mutual coupling between two mobile phone PIFAs operating in the DCS1800 and UMTS bands," *IEEE Trans. Antennas Propag.*, vol. 54, Nov. 2006.

[11] H. Wang and M. Zheng, "Input impedance-tuning slots of PIFA antennas," in *Proc. EuCAP*, Nov. 11–16, 2007, pp. 1–4.

[12] C. R. Rowell, A. C. K. Mak, and C. L. Mak, "Isolation between multiband antennas," in *Proc. IEEE APS/URSI/AMEREM Int. Symp.*, Albuquerque, NM, Jul. 2006, pp. 551–551.

[13] C. R. Rowell and R. D. Murch, "A capacitively loaded PIFA for compact mobile telephone handsets," *Proc. IEEE Trans. Antennas Propag.*, vol. 45, no. 5, pp. 837–842, May 1997.

[14] Z. Ying and A. Dalhstorm, "Some important antenna innovations in the mobile terminal industry in the last decade," presented at the EuCap, Nice, France, Nov. 2006.

[15] L. J. Foged, L. Duchesne, L. Durand, F. Herbiniere, and N. Gross, "Small antenna measurements in spherical nearfield systems," in *Proc. EuCAP*, Nov. 11–16, 2007, pp. 1–4.

[16] R. Garg, P. Bhartia, I. Bahl, and A. Ittipiboon, *Microstrip Antenna Design Handbook*. Norwood, MA: Artech House, 2001.

[17] J.-S. Hong, *Microstrip Filters for RF/Microwave Applications*, 2nd ed. Hoboken, NJ: Wiley, 2011.

[18] D. H. Kwon, "Effect of antenna gain and group delay variations on pulse-preserving capabilities of ultrawideband antennas," *IEEE Trans. Antennas Propag.*, vol. 54, no. 8, pp. 2208–2215, Aug. 2006.

[19] W. Gong, D. R. Jackson, J. T. Williams, and J. T. , "Phase and group delays for circularly-polarized microstrip antennas," in *Proc. IEEE APS/URSI/AMEREM Int. Symp.*, Albuquerque, NM, Jul. 2006, pp. 1537–1540.

[20] S. Blanch, J. Romeu, and I. Corbella, "Exact representation of antenna system diversity performance from input parameter description," *IET Electron. Lett.*, vol. 39, no. 9, pp. 705–707, 2003.

Corbett Rowell (S'95–M'97) received the B.A. degree in physics from the University of California, Santa Cruz, in 1994, and the M.Phil. EEE degree from Hong Kong University of Science and Technology, in 1996. He is currently pursuing the Ph.D. degree at Hong Kong University.

From 1997 to 1999, he worked as an RF Engineer at Allgon Mobile Communications in Sweden. In 1998, he started his own antenna design company, Integra Antennas Ltd. and sold part of it in 2003 to Molex Inc. From 2001 to 2003, he worked on Wall Street at JP Morgan as a Technical Expert in venture capital. From 2003 to 2005, he was a Senior Antenna Engineer at Molex Inc. in Hong Kong. Currently, he is the R&D Director of RF Systems at the Applied Science and Technology Research Institute in Hong Kong. He has published 10 papers with almost 500 citations and holds 35 patents. His research interests are digital-RF, FPGA, miniature antennas, antenna arrays, active antennas, beam-forming, isolation, and sensor arrays.

Edmund Y. Lam (S'97–M'00–SM'05) received the B.S., M.S., and Ph.D. degrees in electrical engineering from Stanford University, Stanford, CA.

After working in the industry for a few years, he joined the Electrical and Electronic Engineering Department at the University of Hong Kong, where he is now an Associate Professor. He has broad research interests around the theme of computational optics and imaging, particularly its applications in semiconductor manufacturing and biomedical systems.

Dr. Lam received the Outstanding Young Researcher Award from the University of Hong Kong in 2008 as the only recipient in engineering that year. Besides his involvement within the university, he is also a Topical Editor of the *Journal of the Optical Society of America A,* an Associate Editor of the IEEE TRANSACTIONS ON BIOMEDICAL CIRCUITS AND SYSTEMS, and has been guest editors for a couple of journals.